MINERAL IDENTIFICATION AND CLASSIFICATION BY COMBINING USE OF HYPERSPECTRAL VNIR/SWIR AND MULTISPECTRAL TIR REMOTELY SENSED DATA

Li Ni [a], *Hua Wu* [b, c, *]

a. Key Laboratory of Digital Earth Science, Institute of Remote Sensing and Digital Earth, Chinese Academy of Sciences, Beijing 100094, China;
b. State Key Laboratory of Resources and Environment Information System, Institute of Geographic Sciences and Natural Resources Research, Chinese Academy of Sciences, Beijing 100101, China;
c. University of Chinese Academy of Sciences, Beijing 100049, China.
* Authors to whom correspondence should be addressed: wuhua@igsnrr.ac.cn

ABSTRACT

The combining of the hyperspectral visible/near-infrared (VNIR) and shortwave infrared (SWIR) data with the hyperspectral thermal infrared (TIR) data has been recognized to be an effective way for the detailed identification and classification of minerals. However, what are the effects of introduction of multispectral TIR data on the minerals identification and classification and how those effects are, are not well studied in the background of the majority of multispectral TIR data. To fully evaluate the effects of the combining of the hyperspectral VNIR-SWIR reflectivity with the multispectral thermal infrared (TIR) emissivity, this paper tries to use the real data to testify the practicability of introduction of multispectral TIR data for the accuracies of mineral identification and classification. Four classifiers are selected in the experiment. Compared with the results using hyperspectral data alone, the introducing of multispectral TIR data in identification and classification has improved accuracies. However, the overall accuracies are improved about 1-5% by using different classifiers. Although those improvements are not well obvious due to the low spatial resolution, where the spectral mixture of various minerals exists, and the retrieval error of land surface emissivity, the multispectral TIR data are still effective supplements for hyperspectral VNIR and SWIR data in mineral identification and classification.

Index Terms—Thermal infrared; classification; emissivity

1. INTRODUCTION

Mineral, as an unrenewable natural resource, has been an important support for the healthy development of economy and society. In the past few years, with a large amount of mineral resources being mined, there are less and less minerals can be found on the surface [1]. A more efficient and accurate method is required to be explored to identify and classify minerals. To realize a wide area of the mineral resources investigation, and overcome some inconvenient transportation and natural conditions of mineral exploration, remote sensing technology, especially for hyperspectral remote sensing, has become a high efficient and convenient method for detecting minerals.

In recent years, much work has been carried out to identify and classify minerals accurately by taking the advantage of hyperspectral data's narrow bandwidth and contiguous spectral [2]. However, minerals' identification remain several problems. Firstly, mineral identification is mainly based on the spectral characteristics in the visible near-infrared (VNIR) bands in 0.4-2.5 μm, and these characteristics are related to certain chemical compositions and lattice structures of minerals [3], while the spectral absorption characteristics in the thermal infrared (TIR) bands are always tend to be overlooked. Secondly, the alteration minerals contain a large number of Fe2+, Fe3+, OH-, $CO_3$2- and other ions or groups of ions. The electronic transition, vibration and rotation of these ions makes minerals display special spectral absorption and reflection characteristics in different spectral bands [4]. Thirdly, the vibration intensity of the minerals cannot be detected across the VNIR-SWIR bands even with hyperspectral data, which limits the ability of mineral indentation and classification. Most abundant minerals have special spectral characteristics in TIR bands in 8-14 μm [5].

To improve mineral identification and classification accuracy and realize fine mapping, some researches have evaluated different classifiers for mineral mapping by using just VNIR-SWIR and TIR data or the combining of those data [6-9]. It has been found that the combined data achieved

a marked improvement compared to the results using either VNIR-SWIR or TIR data alone [6-7,9]. The TIR data used by those researches are usually hyperspectral data with tens to hundreds of channels, in which the mineral features will be well captured. It is may not be a problem for airborne platforms because many sensors have this ability. By contrast, the spaceborne sensor usually has a fewer TIR channels especially for high resolution sensors. The limited spectral channels may influence the mapping accuracies. The use for multispectral TIR data, especially for spaceborne sensor with a few channels, has not been well studied. This paper tries to fully evaluate the effects of the combining of the hyperspectral VNIR-SWIR reflectivity with the multispectral thermal infrared (TIR) emissivity on the accuracies of mineral identification and classification by using the real data.

2. METHODOLOGY

2.1 Spectral diagnosed characteristics of mineral in VNIR/SWIR/TIR

Different minerals have their own specific spectral features and characteristics in VNIR/SWIR/TIR bands, which are closely related to its intrinsic physical and chemical properties. Those special spectral absorption and reflection features and characteristics are reported to be the reason of the electronic transition, vibration and rotation of ions. The different spectral absorption and reflection features and characteristics in VNIR, SWIR and TIR are shortly listed in Table 1.

Table 1. Minerals identified in different wavelength bands.

Region	Wavelength range	Minerals or groups of ions
VNIR	0.40-1.20 um	Fe, Mn and Ni oxide, hematite, goethite
SWIR	1.30-2.50 um	Hydrate, carbonate and sulfate
	1.47-1.82 um	Sulfates, such as alunite
	2.16-2.24 um	Minerals containing Al-OH groups of ions, such as kaolinite
	2.24-2.30 um	Minerals containing Fe-OH groups of ions, such as jarosite
	2.26-2.32 um	Carbonates, such as calcite, dolomite
	2.30-2.40 um	Minerals containing Mg-OH groups of ions, such as talc
TIR	8.00-14.0 um	Quartz, felspar, chalcedony, calcite, dolomite

2.2 Review of four selected classifiers

To evaluate how the accuracies of classification change when TIR data are introduced in mineral identification and classification, four traditional classifiers, i.e. spectral angle mapping (SAM), spectral feature fitting (SFF), orthogonal subspace projection (OSP) and adaptive coherence/cosine estimator (ACE), are used in the following experiment.

The SAM classifier determines spectral similarity between the test spectra and reference spectra by treating them as vectors in an N-dimensional space [10]. The similarity of the two spectra is determined by calculating the angle between the two vectors in the N-dimensional space. The SFF classifier that sensitive to the subtle mineral absorption features is used for spectral analysis about recognition and classification, which is based on spectral absorption features [11]. The OSP classifier is based on a linear spectral mixture model, which divides the mixed pixels into interest target endmember and non-interest background endmember. The mineral is identified by enhancing the characteristics of the target and suppressing the background signatures [12]. The ACE classifier takes both the statistical model and subspace projection model into account. The similarity between the test spectra and the reference spectra is determined by calculating the cosine square of the angle between two spectra [13].

3. DATA

The study area is the Cuprite mine in Nevada, USA. The corresponding hyperspectral AVIRIS reflectivity data in VNIR/SWIR bands and the multispectral ASTER emissivity data in TIR bands were used. The AVIRIS VNIR/SWIR data was acquired on September 20th 2006 and the ASTER TIR data were acquired on August 15th 2006. Because there is a spatial resolution difference between VIR/SWIR data (15.7m) and TIR data (90m), spatial registration is first carried out to keep the two data in the same geographical coordinates. The main minerals of study area consist of alunite, kaolinite, montmorillonite, white mica, chalcedony and so on (Figure 1). The black colour indicated unclassified class. Figure 1 will be used as the ground truth data for assessing classification accuracy.

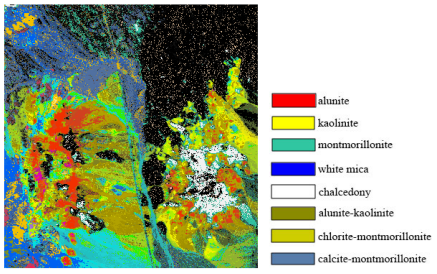

Figure 1. The mineral distribution in studied area

Figure 2 shows the reflectivity of selected minerals in the VNIR/SWIR band and the emissivity in the TIR band respectively. Those spectra are gotten from the average spectra of the minerals in the ground truth data. The spectral differences in both VNIR/SWIR band and TIR band are not obvious.

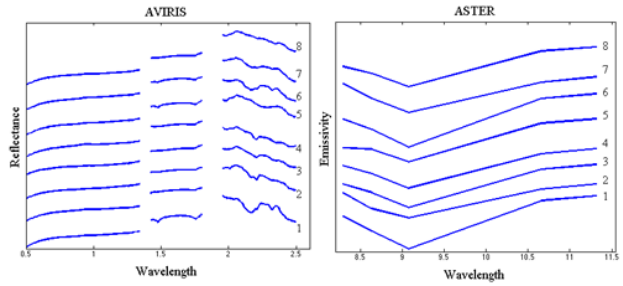

Figure 2. The reflectivity and emissivity (offset for clarity) of eight targets. (1-alunite, 2-kaolinite, 3-montmorillonite, 4-white mica, 5-chalcedony, 6-alunite-kaolinite, 7-chlorite-montmorillonite, 8-calcite-montmorillonite)

4. RESULTS

Four classifiers are used to identify minerals with real AVIRIS data and the combination of AVIRIS and ASTER thermal infrared data. The accuracy of classification is shown in Table 2. The overall classification accuracy of those four classifiers are improved from 1% to 5%. Obviously, the most accurate classifier is SFF, followed by SAM and ACE, and the OSP classifier is not qualified. There may be two reasons according to our analysis. One is related to the quality of data, and the other is related to the principle of classifier. Both SAM and SFF depend on spectral similarity between training samples and targets to be classified, SAM emphasizes on spectral shape, while SFF emphasizes on spectral absorption characteristics. For the real data, the differences in minerals' spectral shape are not obvious compared with the difference in spectral absorption, the overall accuracies of SFF is better than those of SAM. However, it is difficult for OSP and ACE classifiers to achieve a good accuracy when the sample spectrum is slightly different from that of the background.

The main reason why the improvement of accuracy is not obvious may be the relative low spatial resolution of ASTER TIR data, where the spectral mixture of various minerals exists. It can be found in Figure 2 that the similarity of each kind of mineral emissivity curves will affect the classification accuracies. In addition, the spectrum mixture of minerals may be nonlinear and complicated. Thirdly, the retrieval accuracies of emissivity in ASTER TIR bands are reported to be about 0.015, which may not be satisfied the required accuracies in classification.

Table 2. Classification accuracies of different minerals using four classifiers for the real data.

	SAM				SFF			
	AVIRIS		Combined		AVIRIS		Combined	
OA	79.27		80.10		81.43		84.59	
Kappa	0.76		0.77		0.78		0.82	
Classes	Prod.	User	Prod.	User	Prod.	User	Prod.	User
1-alunite	90.51	98.00	90.39	97.99	82.51	98.43	91.52	97.96
2-kaolinite	78.10	92.39	78.66	92.24	80.97	85.01	86.67	84.24
3-montmorillonite	89.53	92.77	90.53	94.95	85.46	87.47	93.37	80.26
4-white mica	89.73	98.84	92.45	99.19	68.88	93.83	77.64	98.09
5-chalcedony	79.75	100.00	80.68	100.00	86.42	100.00	82.88	100.00
6-alunite- kaolinite	44.84	54.86	46.45	56.57	84.30	89.29	85.84	92.42
7-chlorite- montmorillonite	68.29	26.57	68.90	27.26	87.79	71.88	73.17	70.80
8-calcite- montmorillonite	96.59	56.24	96.59	57.52	68.80	100.00	68.94	95.82

	OSP				ACE			
	AVIRIS		Combined		AVIRIS		Combined	
OA	45.25		50.83		76.17		81.78	
Kappa	0.39		0.45		0.73		0.79	
Classes	Prod.	User	Prod.	User	Prod.	User	Prod.	User
1-alunite	47.82	78.15	50.75	85.00	61.13	88.35	67.64	95.94
2-kaolinite	76.79	97.63	74.09	97.07	89.38	96.77	92.64	98.81
3-montmorillonite	33.89	17.06	37.87	19.79	83.89	98.25	76.08	99.57
4-white mica	49.55	65.08	41.84	58.81	87.92	98.15	87.01	98.80

5-chalcedony	43.17	98.33	60.83	98.70	72.95	99.36	81.95	99.76
6-alunite- kaolinite	8.70	25.99	21.57	53.40	70.48	95.88	89.50	92.02
7-chlorite- montmorillonite	46.34	17.82	53.66	21.10	68.90	56.22	66.77	77.94
8-calcite- montmorillonite	59.72	75.44	58.72	53.18	99.80	84.26	98.80	93.73

5. CONCLUSIONS

This paper analyses the spectral characteristics of the reflectivity spectra in VNIR/SWIR and the emissivity spectra in TIR for minerals. The reflectivity of AVIRIS data and the emissivity of ASTER data in Cuprite, Nevada, USA are used in the experiment. With the different kinds of minerals, four classifiers are also used to identify the effect of the combination of hyperspectral VNIR/SWIR data and multispectral TIR data. The real data have proven that the combination of hyperspectral VNIR-SWIR data and multispectral TIR data has a positive impact on the identification and classification of minerals. However, the overall classification accuracy of those four classifiers are improved from 1% to 5%. Some classifiers, such as ACE and SAM, show unobvious difference in classification accuracies because of the slight contrast between target and background spectra. The possible reasons of minor improvements are summarized as follows: 1) the spatial resolution of ASTER TIR data is 90m, which is much lower than expectation. It is easy to cause mixture pixels; 2) the retrieved accuracy of emissivity in TIR band and we argued what is the required accuracy of emissivity in classification. Apparently, the accuracy of retrieved emissivity directly affect the accuracy of classification; 3) the potential nonlinear mixture of mineral complicates the improvement of classification. Although the classification improvement is not obvious, it is still shown that there is a good potential of introducing the multispectral TIR data. The multispectral TIR band data will be appropriate for mineral classification and classification as the complementary of hyperspectral VNIR/SWIR data.

6. AKNOWLEDGEMENTS

This work was supported partly by the National Natural Science Foundation of China under grant Nos. 41771398, 41871267 and 41401394.

7. REFERENCES

[1] N. Gila, V. Kopačková, P. Rojík, S. Guy, L. Ido, and D. Eyal, "Mineral Classification of Land Surface Using Multispectral LWIR and Hyperspectral SWIR Remote Sensing Data. A Case Study over the Sokolov Lignite Open-Pit Mines, the Czech Republic." Remote Sensing 6(8):7005-7025, 2014.

[2] N. Ramesh, S. Amba, and H. Ramesh, "EXhype: A tool for mineral classification using hyperspectral data." ISPRS Journal of Photogrammetry and Remote Sensing 124:106-118, 2017.

[3] E. Cloutis, "Review Article Hyperspectral geological remote sensing: evaluation of analytical techniques." International Journal of Remote Sensing 17(12):2215-2242, 1996.

[4] T. Zhang, and F Liu, "Application of Hyperspectral Remote Sensing in Mineral Identification and Mapping." 2nd International Conference on Computer Science and Network Technology: 103-106, 2012.

[5] A. Charlotte, J. Liu, and J. Philippa, "Hyperspectral remote sensing for mineral exploration in Pulang, Yunnan Province, China." International Journal of Remote Sensing 32(9): 2409-2426, 2011.

[6] X. Chen, T. Warner, and D. Campagna, "Integrating visible, near-infrared and short wave infrared hyperspectral and multispectral thermal imagery for geologic mapping: simulated data." International Journal of Remote Sensing. 28:2415-2430, 2007.

[7] X. Chen, T. Warner, and D. Campagna, "Integrating visible, near-infrared and short-wave infrared hyperspectral and multispectral thermal imagery for geological mapping at Cuprite, Nevada." Remote Sensing of Environment 110:344–356, 2007.

[8] M. Black, T. Riley, G. Ferrier, A. Fleming, and P. Fretwell, "Automated lithological mapping using airborne hyperspectral thermal infrared data: a case study from anchorage island, Antarctica". Remote Sensing of Environment, 176, 225-241, 2016.

[9] J. Feng, D. Rogge, and B. Rivard, "Comparison of lithological mapping results from airborne hyperspectral VNIR-SWIR, LWIR and combined data". International Journal of Applied Earth Observation & Geoinformation, 64:340–353, 2018.

[10] F. Kruse, A. Lefkoff, and J. Dietz, "Expert System-based Mineral Mapping in Northern Death Valley, California/Nevada, using the Airborne Visible/Infrared Imaging Spectrometer (AVIRIS)." Remote Sensing of Environment 44(2-3): 309-336, 1993.

[11] R. Clark, A. Gallagher, and G. Swayze, "Material absorption band depth mapping of imaging spectrometer data using a complete band shape least-squares fit with library reference spectra. Proceedings of the Second Airborne Visible/Infrared Imaging Spectrometer (AVIRIS) Workshop." JPL Publication 2: 4-5, 1990.

[12] J. Harsanyi, and C. Chang, "Hyperspectral image classification and dimensionality reduction: an orthogonal subspace projection approach." IEEE Transactions on Geoscience & Remote Sensing 32(4):779-785, 1994.

[13] S. Kraut, and L. Scharf, "The CFAR Adaptive Subspace Detector is a Scale-Invariant GLRT." IEEE Transactions on Signal Processing 47(9):2538-2541, 1999.